

## Behavioral Analysis of Hydrogen in Metals under the Effect of H<sub>2</sub>S Corrosion Using a Layer-stripping Micro-hardness Technique

Lei GU\*, Jing WANG, Xiaoyang LI

Department of Mechanical Engineering and Applied Electronics Technology, Beijing University of Technology, 100 Pingleyuan, Chaoyang District, Beijing, 100124, P.R. China

**crossref** <http://dx.doi.org/10.5755/j01.ms.26.3.22103>

Received 20 November 2018; accepted 26 February 2019

In order to study the distribution behavior of hydrogen in metals under the condition of H<sub>2</sub>S corrosion, a layer-stripping micro-hardness test was designed to analyze the hydrogen distribution along the depth of hydrogen-charged 45 high-quality structural carbon steel at three different hydrogen sulfide concentrations and four corrosion periods in this study. The results show that there is a terminal solid solubility of hydrogen in the metal for hydrogen sulfide solutions over various concentrations and corrosion periods. A hydrogen-saturated layer is produced by hydrogen diffusing through the metal from an unsaturated state to a fully saturated state. The hydrogen-saturated layer is not affected by the concentration of the corrosion, but its thickness increases as the corrosion period increases. In this way, we established a new hydrogen diffusion model in metals.

**Keywords:** hydrogen distribution, layer-stripping micro-hardness method, terminal solid solubility of hydrogen, hydrogen-saturated layer.

### 1. INTRODUCTION

Many industrial disasters are caused by hydrogen damage to metal. Therefore, research on hydrogen damage to metal in the hydrogen environment is necessary. Hydrogen is a ubiquitous element that enters metal materials from many different sources. Once metals are exposed to hydrogen, they may interact with it resulting in various kinds of structural damage, e.g., hydrogen environment assisted cracking [1], delayed hydride cracking (DHC) [2], and hydrogen embrittlement [3, 4]. The exact assessment of hydrogen concentration behavior is the crux of the study of hydrogen damage in metals. Thus, many researchers have been interested in the hydrogen distribution behavior in metals [5–7], especially recently [8, 9]. In general, there are three kinds of studies of the non-homogeneous hydrogen distribution in academic settings.

First, the non-homogeneous distribution of hydrogen along the depth of hydrogen-saturated specimens is tested using secondary ion mass spectrometry (SIMS) and other methods [10–13]. Second, non-homogeneous hydrogen diffusion can be calculated using a solution of Fick's second law for a semi-infinite plate [14–16]. The diffusion coefficient of hydrogen can be determined using the gas permeation method, electrochemical hydrogen permeation method [17, 18], hydrogen release method, or Gorsky effect method. Third, non-homogeneous hydrogen distribution along the depth was investigated using numerical analyses [19–21].

Currently, many researchers have proven that Vickers hardness increases as the hydrogen content increases in metals [22–27]. Quite a few researchers have proven that the determination of hydrogen diffusivities in materials by subscale micro-hardness profiling is a versatile technique

that can be used to obtain hydrogen diffusivities with simple experimentation [28–33]. The general conclusion of the researchers is: there is a possibility that the local hydrogen concentration behavior can be evaluated through variation of the micro-hardness increment detected by a hardness test employing a universal indentation hardness tester. Micro-hardness is a nondestructive testing method that has been widely adopted and used in the characterization of the mechanical behavior of materials at a small scale.

Based on previous work, a layer-stripping micro-hardness method was designed to analyze the non-homogeneous hydrogen distribution in the direction of depth of the hydrogen-charged 45 high-quality structural carbon steel over different concentrations of H<sub>2</sub>S corrosion and corrosion periods. 45 high quality structural carbon steel is a common quenched and tempered structural medium carbon steel and is widely used in mechanical manufacturing in China. The steel can reflect the hydrogen distribution behavior in metals more accurately than corrosion-resistant steel. The distribution law of hydrogen in an under-saturated state, which has not reached the fully saturated state during the hydrogen diffusion process in metal, was analyzed by studying the micro-hardness changes over the specimen depth with layer-stripping. The depth variations of the experimental hydrogen concentration distribution were compared to theoretical values obtained using Fick's second law.

### 2. THEORY

#### 2.1. Relationship between micro-hardness and hydrogen concentration behavior

To date, many researchers have already proven that the Vickers hardness increases with increasing hydrogen

\* Corresponding author. Tel.: +86-188-1085-6180.  
E-mail address: [audreygulei@foxmail.com](mailto:audreygulei@foxmail.com) (L. Gu)

concentration in metal [22–27]. Some researchers have studied the distribution of micro-hardness in the depth direction of hydrogen-charged specimen, and proven that there is a possibility that the local hydrogen concentration behavior can be evaluated through variation of the micro-hardness increment detected using a hardness test with a universal indentation hardness tester.

Kumar *et al.* [28] proposed the formula where the increase of hydrogen content is proportional to an increase of hardness:

$$\frac{HV - HV_b}{HV_s - HV_b} = \frac{c - c_b}{c_s - c_b}, \quad (1)$$

where  $HV_s$  is the surface hardness of the diffusing species;  $HV_b$  is the bulk hardness of the diffusing species;  $HV$  is Vickers hardness of the diffusing species at any point;  $c_s$  is the surface hydrogen concentration of the diffusing species;  $c_b$  is the bulk hydrogen concentration of the diffusing species, and  $c$  is the hydrogen concentration of the diffusing species at any point.

Hosoda *et al.* [29], Ansari *et al.* [30], and Li *et al.* [31–33] also investigated the quantitative relationship between the hydrogen content and hardness, proving Eq. 1 was correct. The micro-hardness distribution method can be used to test the hydrogen diffusion coefficient in metal.

## 2.2. Mathematical model of hydrogen diffusion and hardness increment

Since  $HV - HV_b = \Delta HV$ ,  $HV_s - HV_b = \Delta HV_s$ , and the hydrogen concentration is zero in the part of the metal without hydrogen, i.e.,  $c_b = 0$ , Eq. 1 can be expressed as follows:

$$\frac{\Delta HV}{\Delta HV_s} = \frac{c}{c_s}. \quad (2)$$

Like most particles, hydrogen atoms move from a high concentration to low when there is a concentration gradient of hydrogen in the crystal or other medium (such as material concentration, stress, or temperature gradients). This movement results in net transport of hydrogen, also called the diffusion of hydrogen.

Fick's first law can be applied to the diffusion problem under the assumption of steady-state. Fick's second law provides more detail, predicting how diffusion causes the concentration to change at any given point in space with time. This law takes the form of a "partial differential equation" and can be applied to the diffusion problem involving both time and space. Therefore, Fick's second law is more applicable to this study.

The rate of hydrogen diffusion can be calculated from a solution of Fick's second law:

$$\frac{\partial c}{\partial t} = D \frac{\partial^2 c}{\partial x^2}, \quad (3)$$

where  $c$  is the hydrogen concentration;  $D$  is the diffusion coefficient of hydrogen;  $t$  is the diffusion time, and  $x$  is the distance to the surface.

Since the boundary conditions for hydrogen diffusion behavior in metals in an environment containing hydrogen

are:  $c(x=0, t=0) = c_{\max}$  and  $c(x>0, t=0) = 0$  [14], the concentration solution of Fick's second law diffusion equation is:

$$c(x, t) = c_s \left[ 1 - \Phi \left( \frac{x}{2\sqrt{Dt}} \right) \right], \quad (4)$$

where  $\Phi \left( \frac{x}{2\sqrt{Dt}} \right) = \frac{2}{\sqrt{\pi}} \int_0^{x/2\sqrt{Dt}} e^{-\xi^2} d\xi$  is the error function introduced in the solution that can be retrieved from a table,  $D$  is the diffusion coefficient,  $t$  is the diffusion time,  $x$  is the distance to the surface.

Combining the concentration solution

$$c(x, t) = c_s \left[ 1 - \Phi \left( \frac{x}{2\sqrt{Dt}} \right) \right] \text{ with } \frac{\Delta HV}{\Delta HV_s} = \frac{c}{c_s}, \text{ Eq. 5 is:}$$

$$\begin{aligned} \Delta HV(x, t) &= \Delta HV_s \left[ 1 - \operatorname{erf} \left( \frac{x}{2\sqrt{Dt}} \right) \right] \\ &= \Delta HV_{\max} \left[ 1 - \operatorname{erf} \left( \frac{x}{2\sqrt{Dt}} \right) \right]. \end{aligned} \quad (5)$$

Although many researchers have been studying hydrogen behavior in metals, the corrosion test period is either too short or too long [12]. The intermediate process for the heterogeneous diffusion of hydrogen into metal has not been completely defined and further studies are still necessary. According to Eq. 5, the maximum hydrogen concentration in metal is determined by  $\Delta HV_s$ . For general metal materials, the maximum hydrogen concentration will never exceed the hydrogen solubility of the material. Therefore, assuming that a given metal has a hydrogen-saturated layer (a layer with a maximum hydrogen concentration (solubility) at any point) under conditions of free diffusion, and the thickness of the layer is  $x_s$ , Eq. 6 can be obtained:

$$\Delta HV(x, t) = \begin{cases} \Delta HV_{\max} & x \leq x_s \\ \Delta HV_{\max} \left[ 1 - \operatorname{erf} \left( \frac{x - x_s}{2\sqrt{Dt}} \right) \right] & x > x_s \end{cases}. \quad (6)$$

## 3. EXPERIMENTAL METHODS

### 3.1. Materials

The investigations were carried out on 45 high-quality structural carbon steel produced by the National Analysis Center for Iron and Steel of China. 45 Steel is a common quenched and tempered structural medium carbon steel in China. The Chinese grade is GB 45#, the corresponding American grade is AISI 1045, the Japanese brand is JIS S45C, and the Germany brand is DIN C45. Cylindrical specimens 12 mm high and 18 mm in diameter were selected. The chemical compositions (mass %) of the tested steel are illustrated in Table 1.

**Table 1.** Chemical composition of the tested steel (mass%)

Steel	C	Si	Mn	S	P	Cr	Ni
45#	0.46	0.27	0.65	0.015	0.018	0.20	0.214

The measured yield strength  $R_{p0.2}$  is 408 MPa and tensile strength  $R_m$  is 714 MPa. The hydrogen diffusion coefficient of the tested steel was determined using the electrochemical hydrogen permeation method, and the value is  $1.18 \cdot 10^{-9} \text{ m}^2 \cdot \text{s}^{-1}$ .

### 3.2. Experimental environment

The specimens were subjected to the micro-hardness test before and after  $\text{H}_2\text{S}$  corrosion at room temperature. Therein,  $\text{H}_2\text{S}$  gas was produced by reaction of a 30 %  $\text{Na}_2\text{S}$  solution with a 30 %  $\text{H}_2\text{SO}_4$  solution. Hydrogen sulfide was dissolved in the National Association of Corrosion Engineers (NACE) test solution A (containing 5 % sodium chloride and 0.5 % glacial acetic acid) [34].

There were three different  $\text{H}_2\text{S}$  concentrations: 800 ppm, 1300 ppm, and 1700 ppm. The  $\text{H}_2\text{S}$  concentrations in the solutions were measured by iodometric titration. In order to avoid developing hydrogen-induced cracks that can affect experimental results, the maximum corrosion period was 96 h according to NACE TM0284–2016 [35], with 24 h, 48 h, and 72 h selected as intermediates. Four corrosion periods were selected to study the hydrogen distribution in metal. 36 specimens were split into 12 groups, each had 3 specimens to ensure accuracy and reliability of the experimental data.

### 3.3. Layer-stripping micro-hardness method

The layer-stripping micro-hardness method is an effective way to detect the hardness distribution curve from the surface to the interior of the specimen after  $\text{H}_2\text{S}$  corrosion.

The initial micro-hardness of the test material was tested before corrosion. After corrosion, the hardness tests were continued using the layer-stripping micro-hardness

method to assess changes in hardness from the surface to the interior of the hydrogen-charged specimens. Starting from the surface, the micro-hardness incremental values were obtained at regular intervals of  $30 \mu\text{m}$  into the specimen.

The layer-stripping of specimens was carried out on a metallographic sample grinder. The particle size of sand paper changed gradually from 400, 800, 1200, 2000 and 3000 until the specimens had a surface mirror effect.

The hardness was measured until the value was stable. The test period of each specimen was slightly less than 1 h.

The hardness test should detect the changes of the material before and after corrosion. In addition, it can also detect the changes along the depth of the specimen. The hardness indicators need to be sensitive enough to assess the material before and after changes in corrosion and depth. For this reason, HV0.2 was used.

The tests in this work were performed using a universal indentation hardness tester Zwick Roell ZHU2.5 according to the national standard GB/T 4340.1 [36]. This standard specifies the principles, symbols and instructions of Vickers hardness test for metals, test equipment, samples, test procedures, uncertainty of results, and test reports.

## 4. EXPERIMENTAL RESULTS

Fig. 1–Fig. 3 show the experimental results obtained using the layer-stripping micro-hardness test. Each point in these figures represents the mean and standard deviation of a measured micro-hardness increment at the same depth of the hydrogen-charged specimens over different concentrations of  $\text{H}_2\text{S}$  corrosion (800 ppm, 1300 ppm, and 1700 ppm) for various corrosion periods (24 h, 48 h, 72 h, and 96 h). The measured micro-hardness changed visibly along the depth due to the presence of hydrogen.

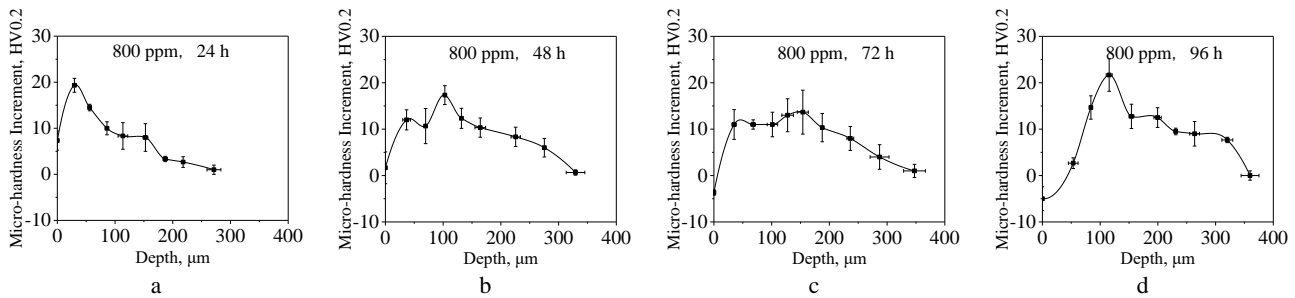


**Fig. 1.** Experimental result of the hydrogen-charged specimens after 800 ppm  $\text{H}_2\text{S}$  corrosion using the layer-stripping micro-hardness test: a – corrosion period of 24 h; b – corrosion period of 48 h; c – corrosion period of 72 h; d – corrosion period of 96 h

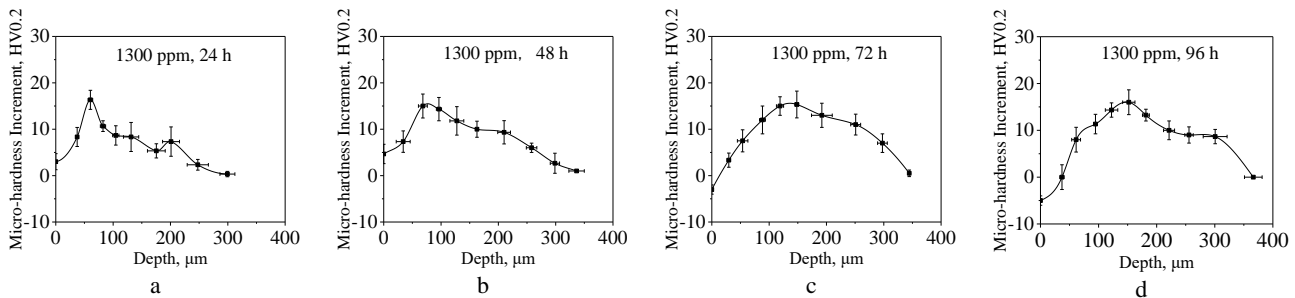


**Fig. 2.** Experimental result of the hydrogen-charged specimens after 1300 ppm  $\text{H}_2\text{S}$  corrosion using the layer-stripping micro-hardness test: a – corrosion period of 24 h; b – corrosion period of 48 h; c – corrosion period of 72 h; d – corrosion period of 96 h

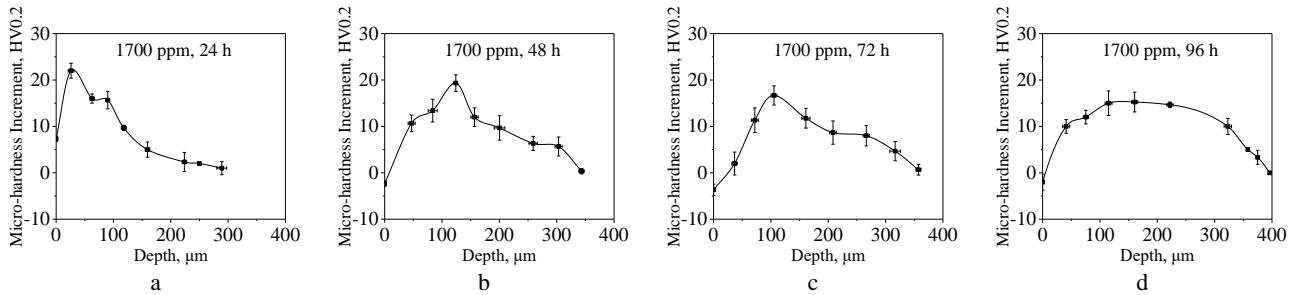


**Fig. 3.** Experimental result of the hydrogen-charged specimens after 1700 ppm H<sub>2</sub>S corrosion using the layer-stripping micro-hardness test: a – corrosion period of 24 h; b – corrosion period of 48 h; c – corrosion period of 72 h; d – corrosion period of 96 h

The trends of distribution curves are all the same, for instance in Fig. 1 a (concentration of corrosion is 800 ppm, corrosion period is 24 h), the micro-hardness increment along the depth increases until it reaches a maximum value at a certain depth, and then it decreases until it returns to zero (restore original micro-hardness  $HV_0$ ). In the most basic form, the distribution of micro-hardness along the specimen depth has three layers. This is to be discussed in the following section.

## 5. DISCUSSION

### 5.1. Terminal solid solubility of hydrogen

Under conditions with different concentrations and corrosion periods, the mean and standard deviation of the maximum increments in the change in micro-hardness of the test specimens for each group are shown in Fig. 4 and Table 2.

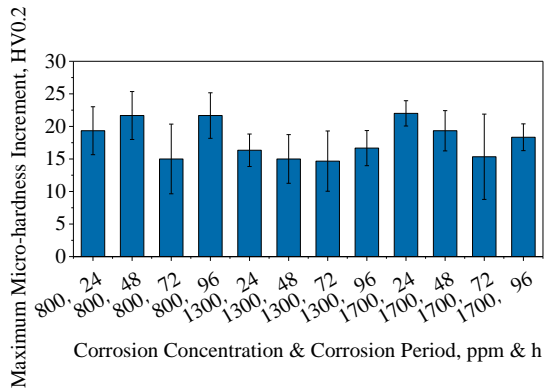


**Fig. 4.** Comparison of the average maximum micro-hardness increment of the hydrogen-charged specimens for each group

The Student's t-test for quantitative variables and Chi-squared test for qualitative variables were used for statistical analysis. There were no statistically significant differences ( $P > 0.05$ ) in the maximum  $\Delta HV_{\max}$  in the hydrogen-charged specimens after H<sub>2</sub>S corrosion over different concentrations and corrosion periods.

Table 2 shows the average maximum micro-hardness increment of 36 test specimens was

$$\overline{\Delta HV_{\max}} = 17.94 \text{ HV0.2.}$$

Because the measured micro-hardness changed in the direction of depth of the hydrogen-charged specimen due to

the presence of hydrogen, and there was a nearly constant value of the maximum micro-hardness increment  $\Delta HV_{\max}$  in the specimens after corrosion, the hydrogen concentration reached a saturated concentration in specimen corresponding to the maximum micro-hardness increment  $\Delta HV_{\max}$ , indicating there was a terminal solid solubility of hydrogen in the hydrogen-charged specimens after H<sub>2</sub>S corrosion over different concentrations and soaking time. The terminal solid solubility of hydrogen was not affected by the concentration of corrosion or corrosion period. The behavioral of hydrogen in hydrogen-charged specimens can be analyzed by the distribution of micro-hardness increment instead of the hydrogen concentration using Eq. 2.

**Table 2.** Micro-hardness test results

	Group	Mean	Standard deviation	n
Corrosion concentration	800 ppm	19.42	3.14	12
	1300 ppm	15.67	0.98	12
	1700 ppm	18.75	2.75	12
Corrosion period	24 h	19.22	2.83	9
	48 h	18.67	3.38	9
	72 h	15.00	0.33	9
	96 h	18.89	2.55	9
Integrated	All	17.94	1.81	36

Note: The  $P$ -value is the probability of obtaining a result at least as extreme as the one that was actually observed, given that the null hypothesis is true. When  $P > 0.05$ , there are no significant differences in micro-hardness increment with different period.

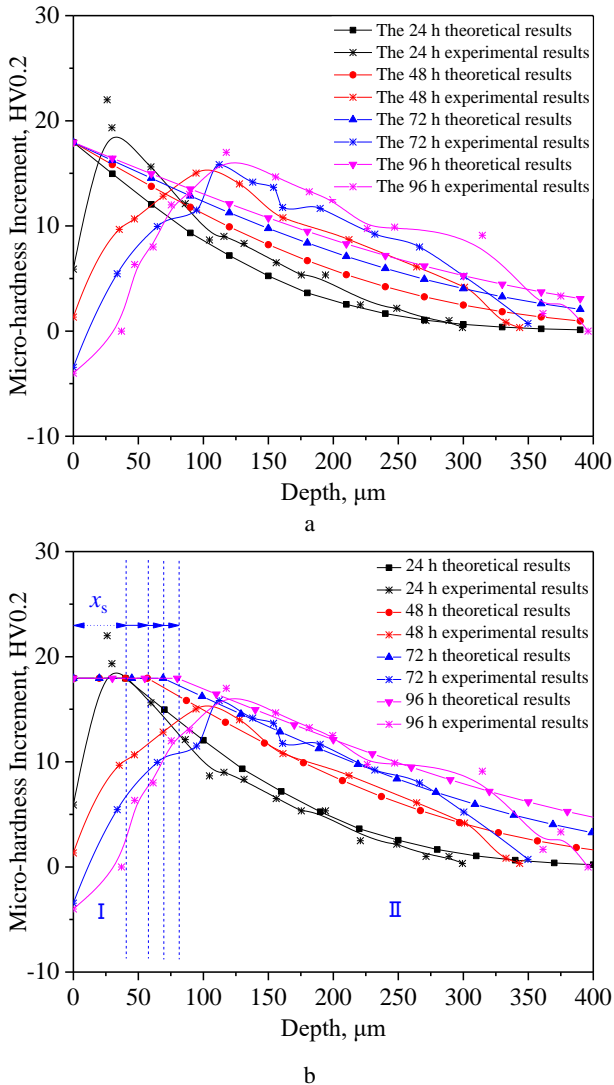
### 5.2. Presence and behavior of the hydrogen-saturated layer

Fig. 5 a shows the depth profiles of theoretical calculated micro-hardness increment using Eq. 5 and the measured results over corrosion periods of 24 h, 48 h, 72 h, and 96 h. The experimental curves were obtained by averaging the distribution of the measured micro-hardness increment distributions acquired from the hydrogen-charged specimens of each corrosion period. Since the experiment results did not change significantly with the three H<sub>2</sub>S concentrations, the hydrogen distribution was not affected by the concentration of corrosion in the experimental observation range.

On the basis of Fick's second law, the theoretical distribution was always from large to small in the direction of depth using a numerical simulation, which is inconsistent with the experimental results shown in Fig. 5 a. There was evident separation between the theoretical curves and the

large-to-small section of the measured results along the depth.

Based on Fig. 5 a, the maximum value was maintained and the theoretical calculated curves move in the direction of depth until the calculated curves coincide with the measured results, with the moving front the maximum micro-hardness increment, as shown in Fig. 5 b.



**Fig. 5.** Depth profiles of theoretical calculated micro-hardness increment and measured result versus corrosion period: a—theoretical curve based on Fick's second law; b—theoretical curve considering of hydrogen-saturated layer

As shown in Fig. 5 b, the theoretical calculated depth profiles after the movement are consistent with the measured depth profiles (Stage II), revealing the presence of a hydrogen-saturated layer (Stage I) in the tested metal. The calculated results are closely consistent with the experimental data, which proves the reliability of both experimental study and numerical analysis.

The saturated layer exists because hydrogen diffusion in metal is a natural diffusion process from high to low. The upper limit of the hydrogen concentration is restricted by the terminal solid solubility of hydrogen in the metal, and the

relationship between time and thickness is affected by the hydrogen diffusion coefficient.

In three previous works [10–12], the hydrogen concentration in the specimens reached saturation after the samples were charged with hydrogen over a sufficiently long period, and the hydrogen concentration remained nearly constant, regardless of the depth of the specimens. In other works [28–33, 37], the distribution of hydrogen concentration in metal changes exponentially from the surface to the interior after a short period of hydrogen charging.

In this study, both the hydrogen-saturated layer and diffusion layer with exponential distribution law exist. As the soaking time  $t$  went on, the hydrogen-saturated layer's thickness  $x_s$  increased, and the micro-hardness increment at the same depth in the diffusion layer also increased (Fig. 6).

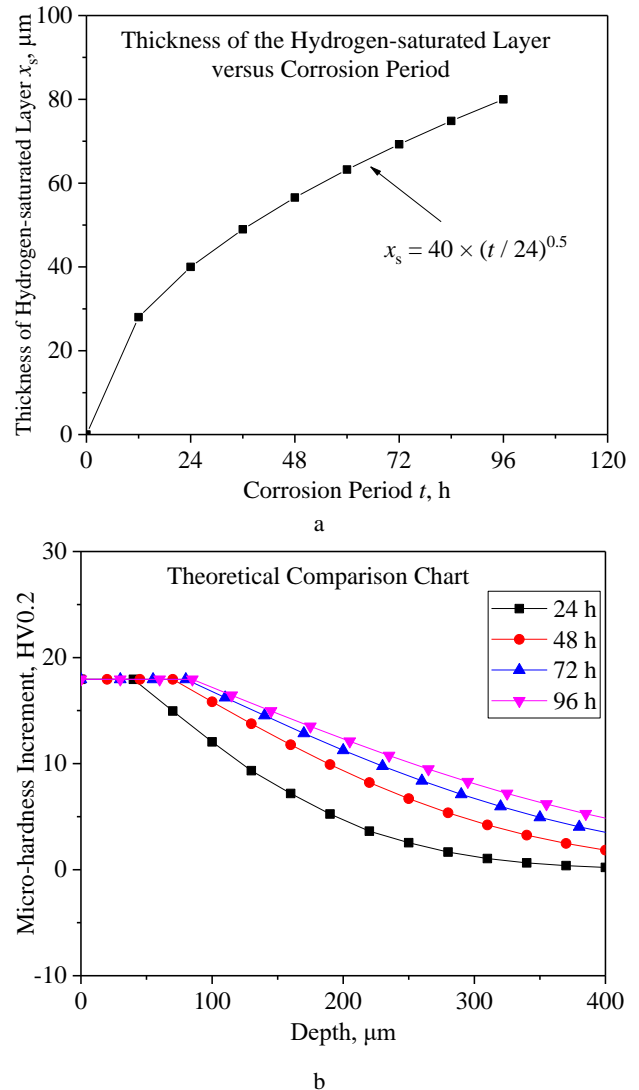


**Fig. 6.** a—thickness of the hydrogen-saturated layer versus corrosion period; b—micro-hardness increment theoretical comparison chart

Given sufficient charging time, the hydrogen distribution in the specimen in the direction of depth tends to be in a saturated state. In this way, results obtained in this study are closely consistent with those of previous studies, which confirms the reliability of the present work.

Because the material used in the research is 45 steel, which is widely used in mechanical manufacturing, the results of this study have universal significance.

Therefore, the hydrogen atoms in the metal diffuse from the unsaturated state to a fully saturated state, the distribution of hydrogen concentration in the metal becomes stratified, producing a hydrogen-saturated layer and hydrogen diffusion layer.

A new model based on Fick's second law is established as shown in Eq. 7, by comparing the hydrogen distribution in metals over different corrosion periods.

$$c(x,t) = \begin{cases} c_{\max} & x \leq x_s \\ c_{\max} \left[ 1 - \operatorname{erf} \left( \frac{x-x_s}{2\sqrt{Dt}} \right) \right] & x > x_s \end{cases} \quad x_s = 40 \times (t/24)^{0.5} \quad (7)$$

Fig. 6 b shows the theoretical calculation depth profiles of micro-hardness increment in the hydrogen-charged specimens after H<sub>2</sub>S corrosion over different corrosion periods using Eq. 7. In Fig. 6 b, with increasing corrosion period, micro-hardness increment increases at the same depth in hydrogen diffusion layer, the absolute value of the slope of the distribution curve decreases, and micro-hardness increment becomes closer to the maximum value along the direction of depth, indicating that the hydrogen distribution in the specimen in the direction of depth tends to be in a saturated state given sufficient time.

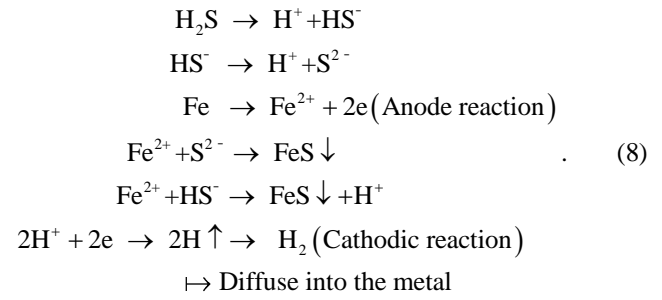
Therefore, the distribution law of hydrogen in the under-saturated state was successfully obtained, also proving that the micro-hardness method can accurately evaluate the degree of hydrogen damage in various metals. This provides a new method for characterizing hydrogen damage.

### 5.3. The difference between theoretical and measured results in the hydrogen-saturated layer (influence of corrosion products in the hydrogen-saturated layer)

Fig. 6 b shows that the values on the theoretical hydrogen-saturated layer curves are constant as an ideal, homogeneous, non-defective metal crystal structure, but the values in the experimental hydrogen-saturated layer curves were not. In Fig. 5 b, the front of the saturated layer of the micro-hardness increments in the experimental curves were found to be lower than the theoretical analysis curves, and they become lower with the closer to the surface of the specimens on the experimental curves. This is because the corrosion of wet hydrogen sulfide in steel is mainly caused by electrochemical corrosion and hydrogen damage from hydrogen diffusing into the steel.

The corrosion products of steel in the hydrogen sulfide aqueous solution are: Fe<sub>9</sub>S<sub>8</sub>, Fe<sub>3</sub>S<sub>4</sub>, FeS<sub>2</sub> and FeS, which can be abbreviated as Fe<sub>x</sub>S<sub>y</sub>. These are generated with a variety of pH conditions and H<sub>2</sub>S concentrations. Fe<sub>x</sub>S<sub>y</sub> is a loose material that can decrease the measured micro-hardness, while hydrogen atoms absorbed by steel could increase the hardness of the metal. Fig. 5 b shows that the measured micro-hardness decreases at the same depth in the hydrogen-saturated layer as the soaking time went on, indicating the corrosion products at the front of the layer increase as the soaking time went on. The mechanism

underlying hydrogen sulfide corrosion was shown in the following equation:



Therefore, the experimental results in the hydrogen-saturated layer are different from the theoretical results. A diagram of hydrogen diffusion in the specimens is shown in Fig. 7. Stage I represents the hydrogen-saturated layer, Stage II represents the hydrogen diffusion layer, and Stage III represents the unaffected layer without hydrogen.

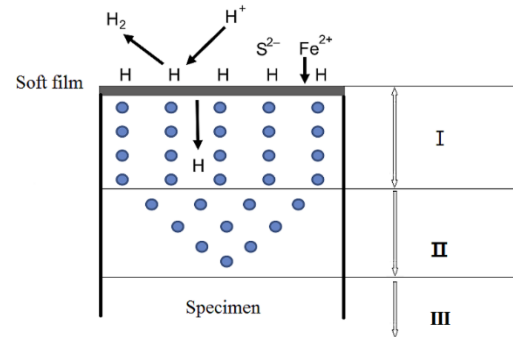


Fig. 7. Diagram of hydrogen diffusion in metal specimens

## 6. CONCLUSIONS

A layer-stripping micro-hardness test of three different hydrogen sulfide concentrations and four different corrosion periods was tested. The hardness distribution in the hydrogen-charged specimen in the direction of depth was captured, indexed, and analyzed. The behavior of hydrogen in the hydrogen-charged specimen was evaluated. Because the material used in the research is 45 steel, which is widely used in mechanical manufacturing, the results of this study have universal significance. The obtained results are summarized below.

1. A terminal solid solubility of hydrogen existed in the hydrogen-charged specimen over different concentrations of corrosion and soaking time, indicating that the hydrogen concentration reached saturation. The terminal solid solubility of hydrogen was not affected by the concentration of corrosion or corrosion period.
2. A hydrogen-saturated layer existed in the hydrogen-charged specimen. As the soaking time went on, the hydrogen-saturated layer's thickness  $x_s$  increased. After the hydrogen-saturated layer, the concentration of hydrogen in the hydrogen-charged specimen gradually decreased in the direction of the depth until it reaches zero. The depth variation of the experimental values is consistent with the calculated values.  $x_s$  was not affected by the concentration of corrosion, only by the

corrosion period.

- The hydrogen-saturated layer exists because hydrogen diffusion in metal is a diffusion process from high to low. The upper limit of the hydrogen concentration is restricted by the hydrogen solubility of the metal, and the relationship between time and thickness is affected by the hydrogen diffusion coefficient. A new hydrogen diffusion model in metals is established.

$$c(x,t) = \begin{cases} c_{\max} & x \leq x_s \\ c_{\max} \left[ 1 - \operatorname{erf} \left( \frac{x - x_s}{2\sqrt{Dt}} \right) \right] & x > x_s \end{cases} \quad x_s = 40 \times (t/24)^{0.5}$$

- The layer-stripping micro-hardness method accurately describes the diffusion behavior of hydrogen in metal.
- Due to the electrochemical corrosion and hydrogen damage by hydrogen atoms diffusing into the steel, the experimental values on the hydrogen-saturated layer curves are not constant in metal.

## Data Availability

The data used to support the findings of this study are available from the corresponding author upon request.

## Acknowledgments

This article is supported by National Key Research and Development Program of China (Project No. 2016YFC0801905-16).

## REFERENCES

- Pioszak, G.L., Gangloff, R.P.** Hydrogen Environment Assisted Cracking of a Modern Ultra-High Strength Martensitic Stainless Steel *Corrosion* 73 (9) 2017: pp. 1132–1156. <https://doi.org/10.5006/2437>
- Coleman, C., Grigoriev, V., Inozemtsev, V., Markelov, V., Roth, M., Makarevicius, V., Kim, Y.S., Ali, K.L., Chakravarty, J.K., Mizrahi, R., Lalgudi, R.** Delayed Hydride Cracking in Zirconium Alloy Fuel Cladding - an IAEA Coordinated Research Programme *Nuclear Engineering and Technology* 41 (2) 2009: pp. 171–178. <https://doi.org/10.5516/NET.2009.41.2.171>
- Pereira, P.A.S., Franco, C.S.G., Filho Guerra, J.L.M., Dos Santos, D.S.** Hydrogen Effects on the Microstructure of a 2.25Cr-1Mo-0.25V Steel Welded Joint *International Journal of Hydrogen Energy* 40 (47SI) 2015: pp. 17136–17143. <https://doi.org/10.1016/j.ijhydene.2015.07.095>
- Neeraj, T., Srinivasan, R., Li, J.** Hydrogen Embrittlement of Ferritic Steels: Observations on Deformation Microstructure, Nanoscale Dimples and Failure by Nanovoiding *Acta Materialia* 60 (13–14) 2012: pp. 5160–5171. <https://doi.org/10.1016/j.actamat.2012.06.014>
- Völkl, J., Alefeld, G.** Hydrogen Diffusion in Metals, in: A.S. Nowick, J.J. Burton, (Eds.), *Diffusion in Solids*. Academic Press, Cambridge, 1975: pp. 231–302. <https://doi.org/10.1016/B978-0-12-522660-8.50010-6>
- Chasse, K.R., Singh, P.M.** Hydrogen Embrittlement of a Duplex Stainless Steel in Alkaline Sulfide Solution *Corrosion* 67 (1) 2011: pp. 15001–15002. <https://doi.org/10.5006/1.3546848>
- Gui, F., Ramgopal, T., Muller, M.G.** Role of Sour Environments on the Corrosion Fatigue Growth Rate of X65 Pipe Steel *Corrosion* 68 (8) 2012: pp. 730–738. <https://doi.org/10.5006/0590>
- Thomas, S., Sundararajan, G., White, P.D., Birbilis, N.** The Effect of Absorbed Hydrogen on the Corrosion of Steels: Review, Discussion, and Implications *Corrosion* 73 (4) 2017: pp. 426–436. <https://doi.org/10.5006/2242>
- Neeraj, T., Srinivasan, R.** Hydrogen Embrittlement of Steels: Vacancy Induced Damage and Nano-Voiding Mechanisms *Corrosion* 73 (4) 2017: pp. 437–447. <https://doi.org/10.5006/2224>
- Awane, T., Fukushima, Y., Matsuo, T., Murakami, Y., Miwa, S.** Highly Sensitive Secondary Ion Mass Spectrometric Analysis of Time Variation of Hydrogen Spatial Distribution in Austenitic Stainless Steel at Room Temperature in Vacuum *International Journal of Hydrogen Energy* 39 (2) 2014: pp. 1164–1172. <https://doi.org/10.1016/j.ijhydene.2013.10.116>
- Yamabe, J., Matsuoka, S., Murakami, Y.** Surface Coating with a High Resistance to Hydrogen Entry Under High-Pressure Hydrogen-Gas Environment *International Journal of Hydrogen Energy* 38 (24) 2013: pp. 10141–10154. <https://doi.org/10.1016/j.ijhydene.2013.05.152>
- Yamabe, J., Takakuwa, O., Matsunaga, H., Itoga, H., Matsuoka, S.** Hydrogen Diffusivity and Tensile-Ductility Loss of Solution-Treated Austenitic Stainless Steels with External and Internal Hydrogen *International Journal of Hydrogen Energy* 42 (18) 2017: pp. 13289–13299. <https://doi.org/10.1016/j.ijhydene.2017.04.055>
- Tupin, M., Martin, F., Bisor, C., Verlet, R., Bossis, P., Chene, J., Jomard, F., Berger, P., Pascal, S., Nuns, N.** Hydrogen Diffusion Process in the Oxides Formed on Zirconium Alloys During Corrosion in Pressurized Water Reactor Conditions *Corrosion Science* 116 2017: pp. 1–13. <https://doi.org/10.1016/j.corsci.2016.10.027>
- Helmut, M.** *Diffusion in Solids*. Springer, Berlin, 2007: pp. 27–53.
- Takakuwa, O., Yamabe, J., Matsunaga, H., Furuya, Y., Matsuoka, S.** Comprehensive Understanding of Ductility Loss Mechanisms in Various Steels with External and Internal Hydrogen *Metallurgical and Materials Science Transactions a-Physical Metallurgy and Materials Science* 48A (11) 2017: pp. 5717–5732. <https://doi.org/10.1007/s11661-017-4323-3>
- Li, J., Oudriss, A., Metsue, A., Bouhattate, J., Feugas, X.** Anisotropy of Hydrogen Diffusion in Nickel Single Crystals: the Effects of Self-Stress and Hydrogen Concentration on Diffusion *Scientific Reports* 7 (45041) 2017: pp. 1–9. <http://doi.org/10.1038/srep45041>
- Devanathan, M.A.V., Stachurski, Z.** The Adsorption and Diffusion of Electrolytic Hydrogen in Palladium *Proceedings of the Royal Society of London* 270 (1340) 1962: pp. 90–102. <http://doi.org/10.1098/rspa.1962.0205>
- Tseng, C.H., Wei, W.Y., Wu, J.K.** Electrochemical Methods for Studying Hydrogen Diffusivity, Permeability, and Solubility in AISI 420 and AISI 430 Stainless Steels *Materials Science and Technology* 5 (12) 1989: pp. 1236–1239. <http://doi.org/10.1179/mst.1989.5.12.1236>
- Tan, T., Du, F., Li, J., Wu, S., Feng, Y.** Finite Element Analysis of Hydrogen Diffusion in Large Forgings *Journal*

- of Plasticity Engineering* 24 (1) 2017: pp. 180–186.  
<https://doi.org/10.3969/j.issn.1007-2012.2017.01.029>
20. **Goto, K., Ozaki, S., Nakao, W.** Effect of Diffusion Coefficient Variation on Interrelation Between Hydrogen Diffusion and Induced Internal Stress in Hydrogen Storage Alloys *Journal of Alloys and Compounds* 691 2017: pp. 705–712.  
<https://doi.org/10.1016/j.jallcom.2016.08.288>
  21. **Ren, F., Yin, W., Yu, Q., Jis, X., Zhao, Z., Wang, B.** Solution and Diffusion of Hydrogen Isotopes in Tungsten-Rhenium Alloy *Journal of Nuclear Materials* 491 2017: pp. 206–212.  
<https://doi.org/10.1016/j.jnucmat.2017.04.057>
  22. **Murakami, Y., Kanezaki, T., Mine, Y.** Hydrogen Effect against Hydrogen Embrittlement *Metallurgical and Materials Transactions a-Physical Metallurgy and Materials Science* 41A (10) 2010: pp. 2548–2562.  
<https://doi.org/10.1007/s11661-010-0275-6>
  23. **Smialowski, M.** Hydrogen in Steel. Pergamon Press, London, 1962: pp. 211–213.
  24. **Nibur, K.A., Bahr, D.F., Somerday, B.P.** Hydrogen Effects on Dislocation Activity in Austenitic Stainless Steel *Acta Materialia* 54 (10) 2006: pp. 2677–2684.  
<https://doi.org/10.1016/j.actamat.2006.02.007>
  25. **El-Amoush, A.S.** An Investigation of Hydrogen-Induced Hardening in 7075-T6 Aluminum Alloy *Journal of Alloys and Compounds* 465 (1–2) 2008: pp. 497–501.  
<https://doi.org/10.1016/j.jallcom.2007.10.126>
  26. **Swieczko-Zurek, B., Zielinski, A., Lunarska, E.** Hydrogen Degradation of Structural Steels in Technical Hydrocarbon Liquids *Materials and Corrosion-Werkstoffe Und Korrosion* 59 (4) 2008: pp. 289–295.  
<https://doi.org/10.1002/mac0.200804082>
  27. **Stepien, K., Kupka, M.** Effect of hydrogen on room-temperature hardness of B2FeAl alloys *Scripta Materialia* 59 (9) 2008: pp. 999–1001.  
<https://doi.org/10.1016/j.scriptamat.2008.07.002>
  28. **Kumar, P., Balasubramaniam, R.** Determination of Hydrogen Diffusivity in Austenitic Stainless Steels by Subscale Microhardness Profiling *Journal of Alloys and Compounds* 255 (1–2) 1997: pp. 130–134.  
[https://doi.org/10.1016/S0925-8388\(96\)02846-0](https://doi.org/10.1016/S0925-8388(96)02846-0)
  29. **Hosoda, H., Yoshimi, K., Inoue, K., Hanada, S.** Effect of Wet Environment on Hardness and Yield Stress of B<sub>2</sub> Fe-Al Alloys *Materials Science and Engineering a-Structural Materials Properties Microstructure and Processing* 258 (1–2) 1998: pp. 135–145.  
[https://doi.org/10.1016/S0921-5093\(98\)00926-5](https://doi.org/10.1016/S0921-5093(98)00926-5)
  30. **Ansari, N., Balasubramaniam, R.** Determination of Hydrogen Diffusivity in Nickel by Subsurface Microhardness Profiling *Materials Science and Engineering a-Structural Materials Properties Microstructure and Processing* 293 (1–2) 2000: pp. 292–295.  
[https://doi.org/10.1016/S0921-5093\(00\)01233-8](https://doi.org/10.1016/S0921-5093(00)01233-8)
  31. **Li, Z., Chen, T., Zeng, Z.** Hydrogen and its Diffusion Coefficient in Stainless Steels During Electrochemically Induced Annealing *Journal of Beijing University of Chemical Technology* 32 (5) 2005: pp. 60–63.  
<https://doi.org/10.3969/j.issn.1671-4628.2005.05.014>
  32. **Zhao, J., Ding, H., Zhao, W., Xiao, H., Hou, H., Li, Z.** Influence of Thermohydrogen Treatment on Microstructural Evolution and Hardness of Ti600 Alloy *Chinese Journal of Materials Research* 22 (3) 2008: pp. 262–268.  
<https://doi.org/10.3321/j.issn:1005-3093.2008.03.008>
  33. **Xiao, H., Zhao, J., Zhao, W., Song, D., Du, G., Ding, H., Wang, Y.** Influence of Hydrogenation on Microstructure and Hardness of Ti6Al4V Alloy *Rare Metal Materials and Engineering* 37 (10) 2008: pp. 1795–1799.  
<https://doi.org/10.3321/j.issn:1002-185X.2008.10.023>
  34. **Gu, L., Li, X.** Hydrogen Damage in Metals. 7th International Conference on Nanomaterials and Materials Engineering *IOP Conference Series: Materials Science and Engineering* 380 (1) 2018: pp. 012016.  
<https://doi.org/10.1088/1757-899X/380/1/012016>
  35. **ANSI/NACE TM0284-2016.** Evaluation of Pipeline and Pressure Vessel Steels for Resistance to Hydrogen-Induced Cracking. National Association of Corrosion Engineers, 2016: pp. 14.
  36. **GB/T 4340.1-2009.** Metallic Materials-Vickers Hardness Test-Part 1: Test Method.
  37. **Chu, W., Qiao, L., Li, J., Su, Y., Yan, Y., Bai, Y., Ren X., Huang, H.** Hydrogen Embrittlement and Stress Corrosion Cracking. Science Press, Beijing, China, 2013: pp. 53.